Int. J. Heat Mass Transfer. Vol. 15, pp. 387–402. Pergamon Press 1972. Printed in Great Britain

HEAT TRANSFER CRISIS DATA WITH STEAM–WATER MIXTURE IN A SIXTEEN ROD BUNDLE

R. EVANGELISTI
Laboratorio Tecnologie Reattori, C.S.N., C.N.E.N., Casaccia, Italy

and

G. P. GASPARI, L. RUBIERA and G. VANOLI
Laboratori, C.I.S.E., Segrate, Milano, Italy

(*Received* 2 *December* 1969 *and in revised form* 3 *September* 1970)

Abstract—The experimental data obtained under the PELCO program on heat transfer crisis (54 point) with vertical upward flow of boiling water in a sixteen rod square bundle are presented.

The experiments were carried out with the CISE IETI-3 heat transfer facility under the following conditions:

geometry: (1) square array of sixteen rods
(2) rod dia.: 1·51 cm
(3) overall heated length: 270 cm
radial power distribution: uniform
axial power distribution: two steps ($\phi_{upstream} = 2\ \phi_{downstream}$; $L_{upstream} = 104$ cm)
specific mass flowrate: 70–160 g/cm²s (seven values)
subcooled water at inlet: (5–75°C subcooling)
test section average pressure: 69 kg/cm² abs.

A brief description both of the test element design and of the experimental plant is given.

A short discussion of critical power results and a comparison with the predictions of some of the available correlations are also reported.

NOMENCLATURE

- D, equivalent diameter [cm];
- G, specific mass flowrate [g/cm²s];
- H, enthalpy [J/g];
- H_{gl}, latent heat of vaporization [J/g];
- L, heated length [cm];
- P, pressure [kg/cm²];
- W, power [kW];
- X, steam quality (by weight).

Greek letters

- θ, temperature [°C];
- Δ, finite difference;
- ϕ, heat flux [W/cm²];
- Ω, cross section flow area [cm²];
- Γ, mass flow [g/s].

Subscripts

- *cr*, critical;
- *g*, gas;
- *i*, refers to heated surface or subchannel;
- *in*, inlet;
- *l*, liquid;
- *o*, outlet;
- *s*, refers to boiling length or power.

1. INTRODUCTION

1.1. ALTHOUGH a large number of heat transfer laboratories are concentrating their activities on the investigation of critical heat flux in rod bundle geometry, because of the considerable importance of this parameter in the design of boiling water reactors (BWR, SGHWR,

CIRENE, HWBR, etc.), the available information is still rather scarce.

This is particularly the case for the plutonium fuel element under development at C.S.N. Casaccia of CNEN for plutonium recycling in boiling water reactors, consisting of a cluster of 64 full length rods, 1·5 cm o.d. and 270 cm long [1]. At the time when the present study was undertaken the only critical heat flux data available with a square lattice bundle were those obtained:

at General Electric with four rods [2] (rod diameter = 1·11 cm, heated length = 91 and 122 cm, uniform axial and radial power distribution);

at General Electric with nine rods [3] (rod diameter 1·11 cm, heated length 76·2 and 152·4 cm, uniform axial power distribution, uniform and non-uniform radial power distribution, hot rod);

at ASEA (Sweden) with 9 rods [4] (rod diameter = 1·17 cm, heated length = 160 cm, uniform axial power distribution, uniform and non-uniform, hot rod, radial power distribution).

From the indicated characteristics it is evident that the configuration was quite different from that considered for the plutonium fuel element (in particular as far as rod length and diameter are concerned).

Now more data are available for 16 rod bundles [15, 16] but still on short test sections (6 ft long).

The experimental investigation devised by CNEN and whose results are presented herewith was aimed at obtaining experimental data in a range appropriate to a plutonium fuel element and simulating as closely as possible its rod length, diameter and axial power distribution. As is well known, the actual reactor axial power distribution is of "inlet peak" type [1], while all the available critical heat flux data rod clusters refer to a uniform axial power distribution. Extrapolation of these data to non-uniform power distribution is far from being established.

1.2. The experimental investigation has been carried out with the CISE IETI-3 heat transfer facility located at Piacenza [5], which can provide the water flow and electrical power needed to carry out critical heat flux experiments under the specified conditions. In particular a 6 MW d.c. conversion unit is available for test element heating which allows experiment to be made with a 16 rod bundles of the same diameter and length as foreseen for the plutonium fuel element reference design.

The extrapolation of the critical heat flux data from a 16 to 64 rod bundle needs of course some care but, in the authors' opinion, this should not be so difficult as might be inferred at first sight, since (1) the present knowledge on this effect is reasonably satisfactory; (2) the 16 rod geometry reproduces significantly the 64 rod geometry [1].

The "inlet peak" axial power distribution has been reproduced with a stepped distribution, the upstream portion of the test section length having a heat flux twice the one relevant to the downstream portion. Of course extrapolation to the case of the skewed cosine needs some care: but in any case the data are of great importance since they are the first, available presently, for square lattice rod bundle with a non-uniform axial power distribution.

1.3. The work described here was carried out from April 1968 to March 1969: the specifications regarding the test section configuration and the test conditions were decided in April 1968 [1]. The test section [6, 14] was completed and mounted at the end of 1968 and the experiments carried out in January and February of 1969.

This report gives a brief description of the test facility as well as of the test section and presents, together with a short comment, the experimental data of critical heat flux.

2. EXPERIMENTAL

2.1. The IETI-3 plant [5] can operate according to different hydraulic schemes: the two adopted for critical power and pressure drop

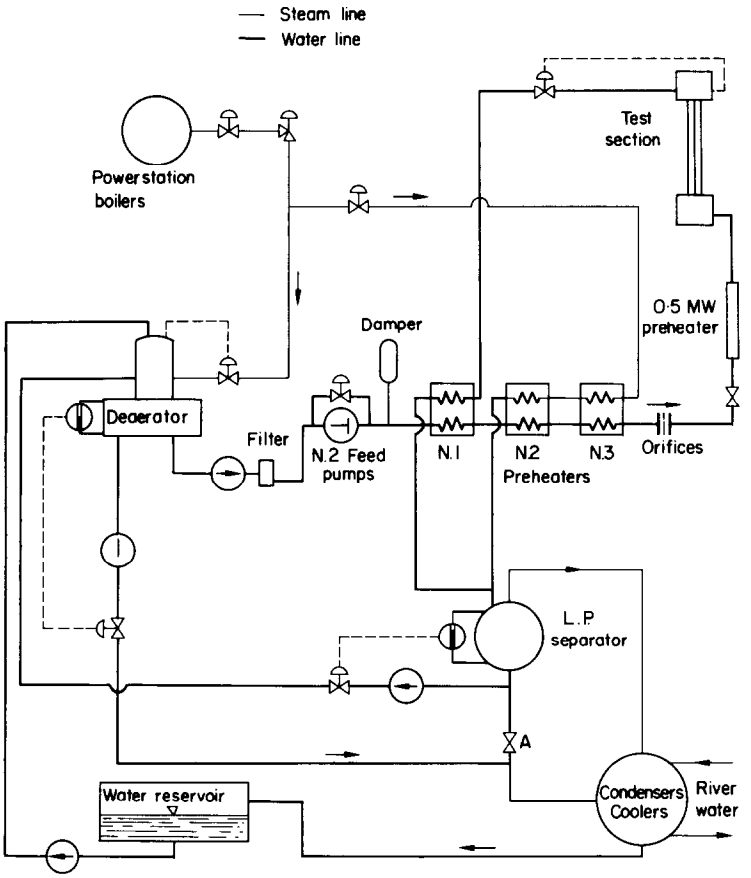

FIG. 1. Hydraulic scheme of the IETI-3 circuit.

tests with the PELCO test element are briefly described here below.

A diagram of the IETI-3 hydraulic circuit is given in Fig. 1.

The plant rating is:

water flowrate	40 m^3/h
steam flowrate	10 t/h
pressure,	70 kg/cm^2 abs
at the test assembly	
d.c. power	7 MW peak service
(at the converter bus-bars)	

On the basis of the required flowrate, the plant operates according to an "open" circuit for flowrate up to 20 t/h), or to a "semi-open" circuit, for which water is recirculated for partial heat and flowrate recovery (for flowrate higher than 20 t/h).

Superheated steam is drawn from the intermediate superheaters of the stations two boilers at 105 kg/cm^2 and 430°C: steam is used for the following purposes:

to deaerate feed water;

to preheat circulation water.

As shown in Fig. 1, demineralized water† provided by the station facilities is sent from a reservoir into a deaerator and, after having been filtered in a resin ion exchanger downstream of deaerator, it is taken to high pressure by means of two reciprocating pumps in parallel (head 120 kg/cm^2; flowrate: 20 m^3/h each). Water enters the heat exchanger (H.E.) No 1, to which heat is supplied from the steam–water mixture

†Water pH value is daily controlled with hydrazine injection.

leaving the test section, it enters H.E. No. 2 and H.E. No. 3 where heat is supplied by superheated steam coming from the boiler. Water is finally sent to the flowrate measuring section, passing through an electric preheater (max: 0·5 MW) and enters the test section.

The steam–water mixture leaving the test section is depressurized through a throttling valve, automatically or manually operated to keep pressure constant at the test element outlet, enters the H.E. No. 1 and then is sent to the low pressure separator.

Downstream of the low pressure separator, water can be discharged either into the river water cooled condenser-coolers, if the plant is operated as an "open" circuit, or directly into the deaerator when the loop is partially closed. In this last case valve A is closed and the deaerator level is kept constant by discharging part of the water into the condenser-coolers.

The change between the open and "semi-open" schemes is simply carried out by means of valves.

The average chemical conditions of the circulating water are:

electrical conductivity	12 μmhos/cm
pH (at room temperature)	8·8
SiO_2	120 γ/litre
NH_3	220–250 γ/litre
Fe^3	400 γ/litre
O_2	none

2.2. The measured quantities for each experiment are: flowrate, water inlet temperature (inlet enthalpy), pressure, pressure drop across the whole test element or a portion of it, electric power, rod wall temperature.

The whole plant instrumentation is as far as possible centralized to allow fast and automatic acquisition of all the interesting readings during experiments. With this purpose the main instrumentation is connected with a Hewlett & Packard data acquisition system, provided with a high precision digital voltmeter together with a twenty-five channel scanning system: the above mentioned readings are then directly printed on a paper strip.

Water flowrate is measured at high pressure upstream of the electrical preheater by means of a set of orifices connected to a mercury column differential manometer. The accuracy reached with these orifices (calibrated from time to time) during the present tests is ± 1–2·5 per cent.

The d.c. power (voltage and current) supplied to the test section is measured directly by the data acquisition system; the total accuracy is better than 1 per cent f.s. (the main error being due to the shunt calibration error).

Inlet and outlet pressures are measured by means of steel blade precision manometers of the Blondelle type (100 kg/cm^2 f.s.) $\pm$ 1 per cent f.s. accuracy.

2.3. Thermopiles, which are placed inside the rods at the downstream ends of the two heated portions, have been used for heat transfer crisis detection. In fact due to the stepped axial heat flux distribution, the crisis might appear either at the downstream end of the upstream section (i.e. of the higher heat flux portion) or more probably (as preliminary calculations seem to indicate) at the outlet heated end. So in these two sections each rod is equipped with thermopiles. They are made of four Ni–Ni Cr thermocouples, 90° spaced from one another inside the rod itself (in a plane), connected in series: thus the crisis which, as observed in other laboratories, spreads more easily in the flow direction than circumferentially over the rods [7], can be quickly detected. Each hot junction of these four thermocouples is located inside a groove worked in a ceramic support contacting the rod wall (see Fig. 2).

In order to make possible, with the available plant instrumentation, the continuous observation of the wall temperature rise in all the rods with increasing power, both the outlet thermopiles of two rods (with the exception of the four corner rods) and the upstream thermopiles of four rods have to be operated in series. These, in their turn, operate differentially† with a Ni–Ni Cr

†This is done in order to avoid too large voltage outputs when many thermopiles operate "in series".

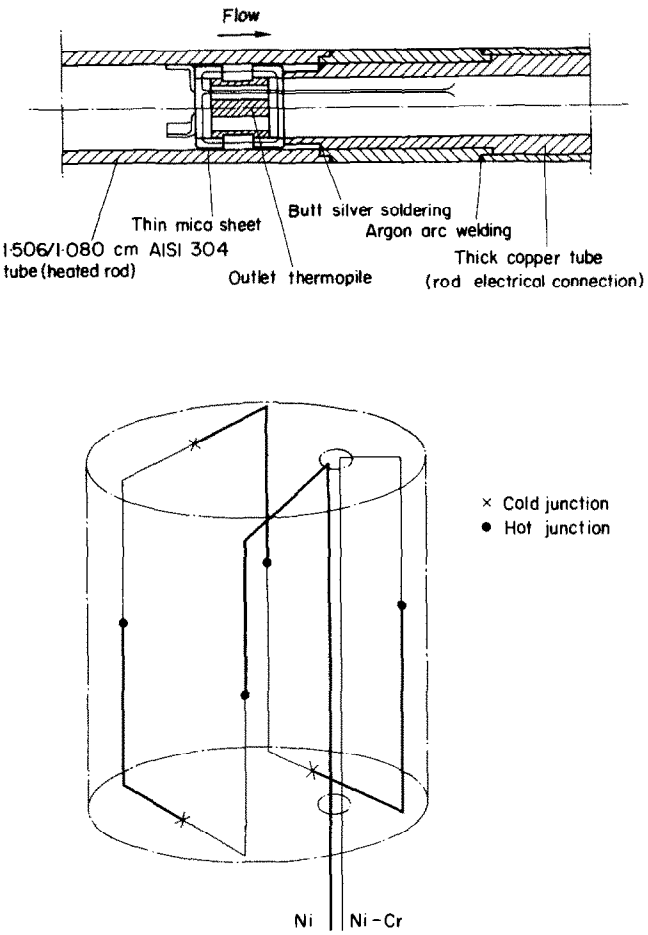

FIG. 2. Thermopile electrical scheme and drawing of rod electrical connection.

thermocouple which, being located on the unheated portion of the outlet line, effectively measures the mixture saturation temperature (Fig. 3).

The differential thermopile outputs ($\Delta\theta$) equal, in a first approximation, to the sum of the metal and film temperature drops, are continuously recorded with the power increase to the test element, in order to observe the start of $\Delta\theta$ fluctuations at crisis onset.

The $\Delta\theta$ values both of the thermocouple outputs of the four corner rods and of twelve other rods, connected two by two, are continuously recorded. Similarly the $\Delta\theta$ values of the upstream thermopile outputs of the sixteen rods, connected four by four, are continuously recorded by two twin-channel potentiometric recorders in order to detect upstream crisis. Since such a crisis (due to the high heat flux and low quality in this section) would be a fast crisis, the thermopile output acts directly on the high voltage circuit breaker to shut off power when rod wall temperature exceeds 600°C. Moreover for upstream and outlet thermopiles a manual

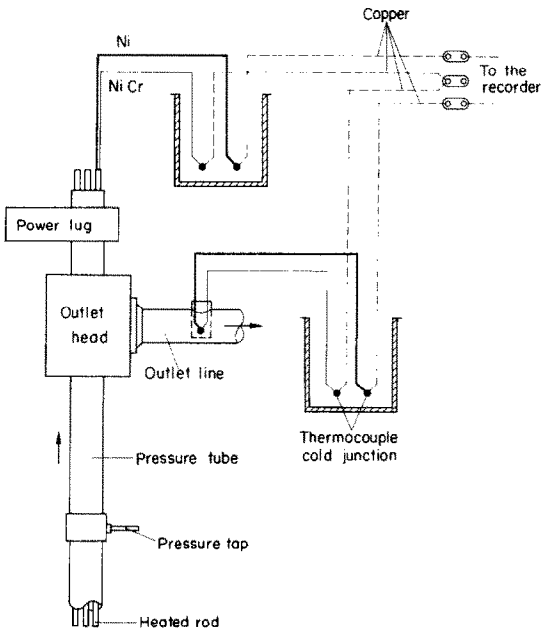

FIG. 3. Differential thermocouple scheme.

scanning device allow additional monitoring of each thermocouple of the series.

All upstream thermopiles have revealed a poor electrical insulation towards the heated wall, consequently $\Delta\theta$ recordings present very strong electrical noise which does not permit any quantitative information about the rod wall temperature in the upstream section (this difficulty did not prevent the use of these thermopiles for crisis detection). On the contrary the behaviour of all outlet thermopiles have proved to be satisfactory, although sometimes they too, present a little electrical noise.

2.4. The sixteen rod bundle called PELCO-IT 33 has the following characteristics:

rod dia.	1·506 cm
rod–rod spacing	0·424 cm
rod–pressure tube spacing	0·364 cm
pressure tube width	8·025 cm
overall heated length (upstream + downstream sections)	270 cm
upstream section heated length	104 cm
downstream section heated length	166 cm
overall pressure tap distance	242 cm
cross flow area	35·02 cm^2
equivalent diameter	1·343 cm
axial power distribution	rectangular (ϕ_{in} $\phi_0 = 2$)
radial power distribution between the rods	uniform
spacers	grid every 48·5 cm

For a detailed description of the test element design as well as of its construction and assembly, reference is made to [14].

The test element has been designed according to the concept already adopted and proved satisfactory for CISE nineteen rod bundle [9]; with this concept the following purposes can be attained:

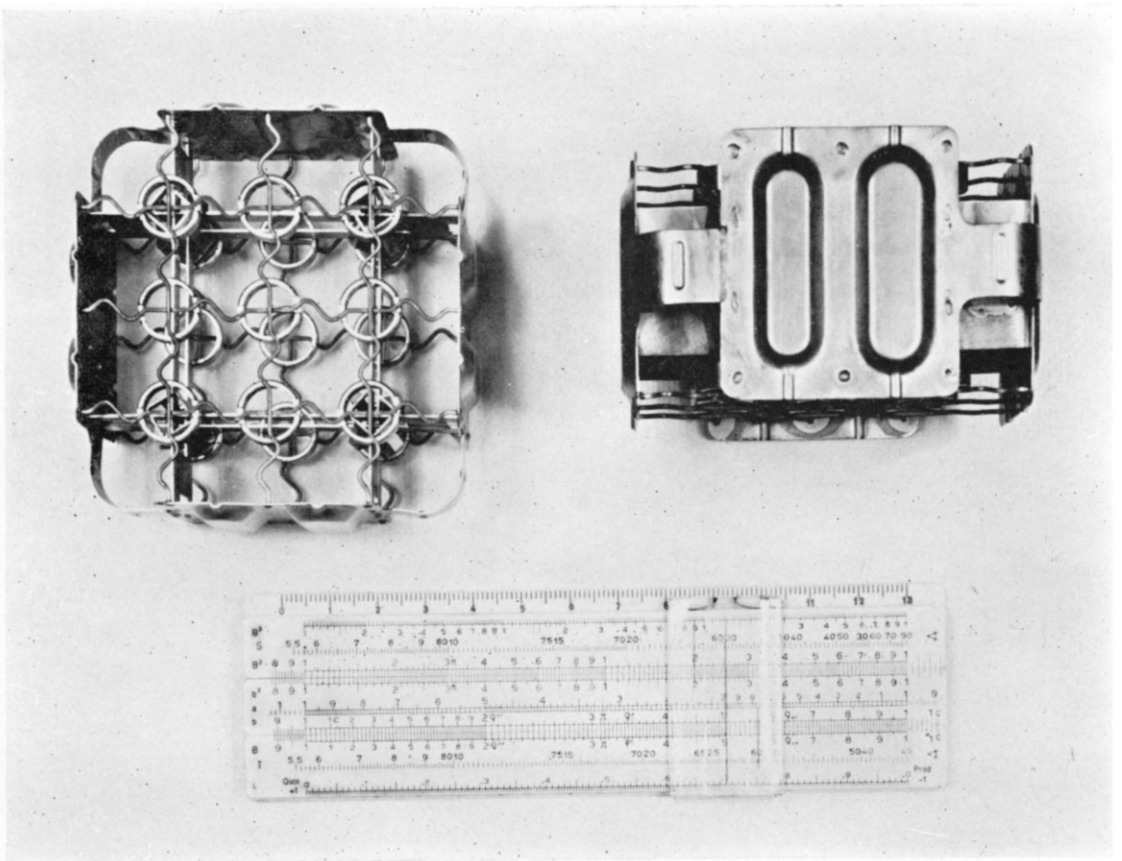

FIG. 4. Picture of the whole pressure tube assembly.

[*facing page 392*]

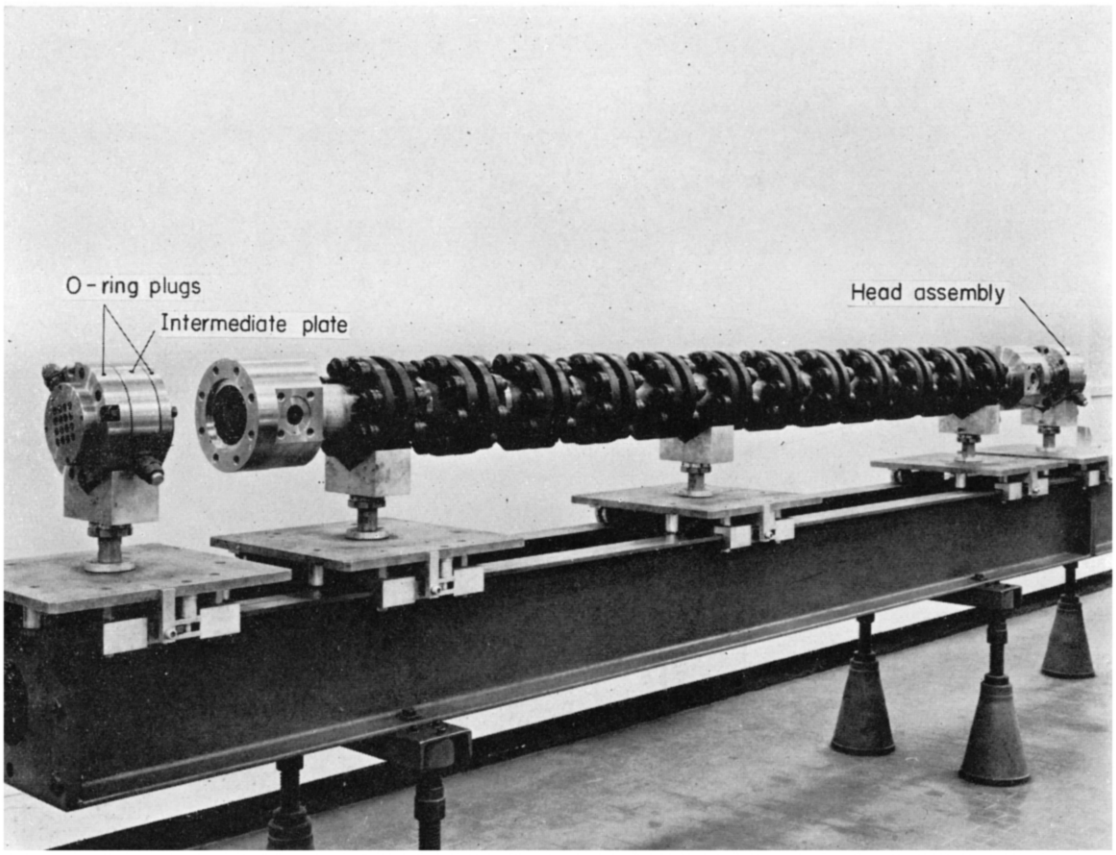

FIG. 5. Grid spacers for the PELCO test element.

(1) the possibility of dismantling the whole test element and in particular the rods (each one independently of the others). This allows substitution of the rods which might fail during the tests;
(2) the possibility of using metallic spacers (grids representing the spacers envisaged for the fuel bundle design) without a short circuit occurring between the spacers and the pressure tube itself. For this purpose a pressure tube has been adopted consisting of different sections, each one electrically insulated from the others.

A picture of the whole pressure tube assembly is presented in Fig. 4. The pressure tube is made of eleven end-flanged AISI 304 stainless steel sections. The sections are electrically insulated one from the other by means of Klingerit gaskets, and are assembled so as to form a continuous straight tube; particular care is given during the assembly to make all sections perfectly coaxial.

The pressure tube assembly is equipped at both ends with two identical heads (Fig. 4). Each head assembly consists of three AISI 304 plates i.e. two O-ring plates and and an intermediate plate which is shaped as to form two water cooled chambers for O-ring cooling. A low pressure water circulation is provided for this purpose.

Each heated rod is made by argon-arc welding together two sections of AISI 304 stainless steel cold drawn seamless tube:

upstream section (towards the inlet): o.d. 1·506 cm, i.d. 1·310 cm, 104 cm long;
the downstream section: o.d. 1·506 cm. i.d.. 1·080 cm, 166 cm long.

In this a way a stepped axial power distribution can be achieved, the heat flux ratio being equal to 2.

At both ends of the heated rod length, two portions of a thick copper tube (1·4/0·6 cm diameters) are inserted into the tube and silver soldered to it as shown in Fig. 2 in order to have good electrical connections and to fix accurately the limits of the heated portion. The power dissipated in the unheated bundle end sections is about 1·7 per cent of total power.

At both ends of the element the rods pass through the O-ring plugs, and are fixed at the top, while at the bottom they can slide to allow thermal elongation.

At both ends electrical connections are made by individual detachable clamps (low pressure water cooled) secured to the rods.

The rod–rod and rod–pressure tube spacings are maintained by metallic spacers (Fig. 5), simulating, on a small scale, the grids for the plutonium fuel element reference design [1]. Since such a grid is smaller in width than the pressure tube, 0·01 cm thin pads (two for each side of the square grid) are spot welded onto grids so as to avoid or minimize vibration in the bundle and to center the whole bundle in the pressure tube.

2.5. Once the required pressure, flowrate and water subcooling are set, the heat transfer crisis is reached by gradually increasing the test element power in a series of steps† until the total rod wall-to-bulk temperature difference $\Delta\theta$ shows the crisis onset. At these conditions all instruments readings are automatically taken through the data acquisition system; power is then decreased by 50 per cent below the crisis value, inlet subcooling is changed and a new test carried out.

Reference [10] describes in detail the qualitative aspects of the type of heat transfer crisis which normally takes place in forced convection with steam water mixture. Critical power is defined as the power input for which a fluctuation affecting the rod wall-to-bulk temperature difference sets in (the fluctuation threshold should be related to the value of the power input at which the disruption of the liquid film cooling the heated wall begins).

According to this definition, the crisis is in general detected by the sudden onset of random

†The size of steps varies but at conditions close to the crisis the steps are such as to give 10–30 kW power increase. Moreover a time interval of 10–20 s is allowed from one step to the other.

temperature oscillations at a point on the heated rod internal wall when electric power is slightly increased.

In our case the fluctuation does not appear and the crisis is defined by a sharp change in the slope of the wall temperature increase.

Regardless of specific mass flowrate, the heat transfer crisis cannot be considered as a fast phenomenon (it needs about 30 s to reach the rod wall temperature equilibrium) and it generally makes excursions of 70–170°C in rod wall temperature.

Some heat transfer crisis measurements were repeated both during the crisis tests and pressure drop measurements to check repeatability of results, which were always in agreement within 2–4 per cent.

3. RESULTS

3.1. The critical power data are presented in the Tables 1–3. The results given in the tables are:

index number of the experiment performed;
†this sign at the side of the number indicates that power has been slightly increased above the first onset of crisis (detected by any single thermocouple);
specific mass flowrate in the test element (G, g/cm^{2}s);
inlet temperature (θ_{in}, °C);
steam quality (by weight) at inlet (X_{in}) and outlet (X_0);
absolute pressure at inlet (P_{in}) and outlet (P_0) (P, kg/cm^2);
critical power (W_{cr}, kW);
critical heat flux in the downstream section (ϕ_2, W/cm^2);
indication of the rod where crisis has been detected;
inner rod wall temperature (θ_w, °C).

Critical power and inlet quality have been selected among the possible variables for the graphic presentation of results in Fig. 6.

† Negative qualities correspond to subcooled water as from $X = H - H_1/H_{gl}$.

3.2. In all the experiments, the crisis always occurs at the outlet end of the heated length notwithstanding the heat flux in the upstream portion is twice that of the downstream portion.

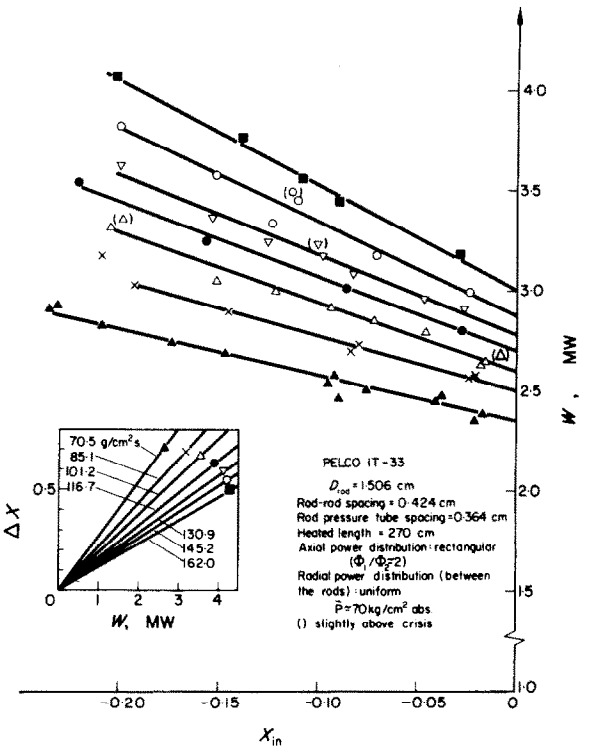

FIG. 6. Heat transfer crisis data.

No experiment has been carried out in order to determine the additional power needed to make crisis to set in at the downstream end of the upstream portion.

This result is in agreement with the conclusion that could be inferred from the application of CISE-3 correlation [11]. As far as the influence of axial heat flux distribution is concerned, this correlation is based on the so-called "global or hydrodynamic condition" hypothesis which states that the heat transfer crisis can be described by an equation between the critical quality and the critical boiling length which is independent from the axial flux shape at con-

Table 1. Critical power PELCO sixteen rod bundle

Run	G (g/cm^{2}s)	θ_{in} (°C)	X_{in} by weight	X_0	P_{in} (kg/cm^2 abs)	P_0	W_{cr} (kW)	θ_2 (W/cm^2)	Crisis on rod	θ_w (°C)
105	69·99	221·8	−0·209	0·554	71·2	71·2	2819	99·27	9	
107	70·93	211·5	−0·231	0·540	69·1	69·1	2914	102·8	9	400
108	70·43	211·2	−0·235	0·541	70·0	70·0	2901	102·2	9	429
109	70·58	230·8	−0·173	9·555	69·4	69·4	2733	96·25	9	408
110	69·46	257·4	−0·090	0·578	69·8	69·8	2463	86·57	9	365
111	69·61	256·2	−0·095	0·592	70·0	70·0	2537	89·26	9	415
112	70·32	278·5	−0·021	0·610	70·2	70·1	2351	82·67	9	
134	71·50	261·7	−0·076	0·583	69·8	69·8	2501	87·42	9	494
135	71·78	279·2	−0·017	0·608	69·8	69·8	2384	83·27	9	491
113	84·92	278·0	−0·024	0·546	70·4	70·4	2564	90·10	9	399
114	85·40	278·2	−0·021	0·546	69·8	69·8	2568	90·41	9	
115	84·80	259·7	−0·084	0·515	70·1	70·1	2693	94·65	9	377
116	85·90	259·9	−0·080	0·517	69·2	69·1	2727	95·80	9	398
117	84·12	239·9	−0·146	0·500	69·7	69·6	2886	101·6	9	411
118	84·17	225·6	−0·193	0·483	70·2	70·1	3016	106·3	9	443
148	86·57	220·0	−0·209	0·480	69·9	69·9	3162	113·5	9	421

Table 2. Critical power PELCO sixteen rod bundle

Run	G (g/cm^{2}s)	θ_{in} (°C)	X_{in} by weight	X_0	P_{in} (kg/cm^{2}abs)	P_0	W_{cr} (kW)	ϕ_2 (W/cm^2)	Crisis on rod	θ_w (°C)
119	102·1	247·1	−0·122	0·429	69·5	69·4	2994	105·6	9	415
120	100·0	221·0	−0·205	0·417	69·7	69·7	3304	116·5	9	437
121	101·4	262·7	−0·072	0·458	69·5	69·4	2857	100·3	9	491
122	100·7	279·2	−0·018	0·474	70·1	69·9	2627	91·97	9	397
123	101·0	279·2	−0·016	0·476	69·6	69·5	2641	92·67	9	413
124	101·4	280·5	−0·009	0·486	68·6	68·5	2676	94·00	9–18	480
147	100·8	223·3	−0·199	0·426	69·9	69·9	3344	120·3	9	526
125	117·9	257·9	−0·086	0·394	69·3	69·2	3016	106·1	9	429
126	116·5	276·2	−0·028	0·425	70·1	69·9	2805	98·55	9–18	457
127	115·9	236·1	−0·157	0·367	69·6	69·6	3232	113·7	9	367
128	116·5	216·5	−0·221	0·350	70·3	70·2	3524	124·2	9	440
130	129·9	246·6	−0·126	0·342	70·1	69·9	3224	113·4	9	423
131	131·2	220·0	−0·200	0·317	69·3	69·2	3607	126·7	9	425
132	129·6	259·9	−0·083	0·364	70·1	69·9	3074	107·8	9	516
133	133·4	275·5	−0·027	0·381	69·1	68·9	2904	101·6	9–18	404

Table 3. Critical power PELCO sixteen rod bundle

Run	G (g/cm^{2}s)	θ_{in} (°C)	X_{in} by weight	Ω_0	P_{in} (kg/cm^2 abs)	P_0	W_{cr} (kW)	ϕ_2 (W/cm^2)	Crisis on rod	θ_w (°C)
129	144·3	247·1	−0·124	0·309	70·1	69·9	3323	116·8	9	447
136	145·1	263·4	−0·071	0·342	70·0	69·7	3177	111·4	9–18	410
137	146·4	277·2	−0·024	0·361	69·7	69·3	2992	104·6	9–18	392
138	144·6	223·5	−0·200	0·297	70·3	70·2	3807	133·5	9–18	466
139	146·4	238·6	−0·152	0·307	70·1	69·9	3563	124·7	9	452
145	145·0	250·6	−0·111	0·336	69·5	69·2	3444	123·7	9	436
146	144·4	249·9	−0·114	0·339	69·7	69·5	3479	125·1	9–18	442
140	161·7	257·9	−0·090	0·311	70·3	69·9	3437	123·2	9–18	459
141	162·6	276·0	−0·029	0·339	70·1	69·6	3176	113·8	9–18	490
142	161·7	242·9	−0·139	0·299	70·3	69·9	3751	123·4	9–18	529
143	161·7	222·8	−0·202	0·271	70·3	69·9	4055	145·5	9	545
144	162·1	251·9	−0·109	0·304	70·0	69·6	3549	127·5	9–18	459

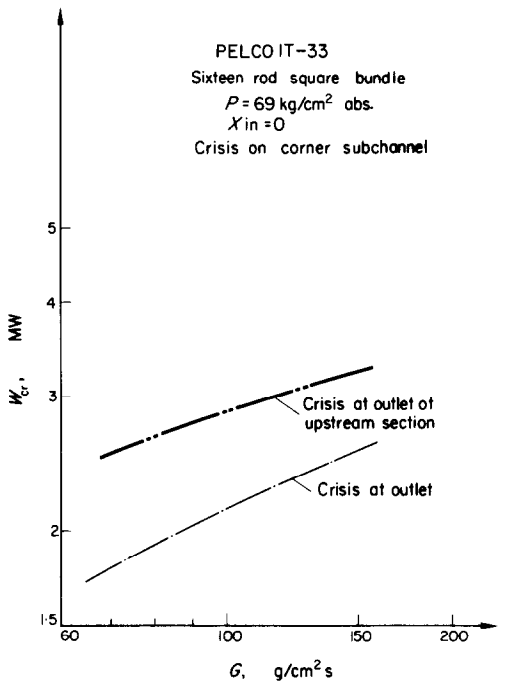

FIG. 7. Total critical power prediction (CISE-3 correlation) for crisis occurring at outlet and outlet of upstream section.

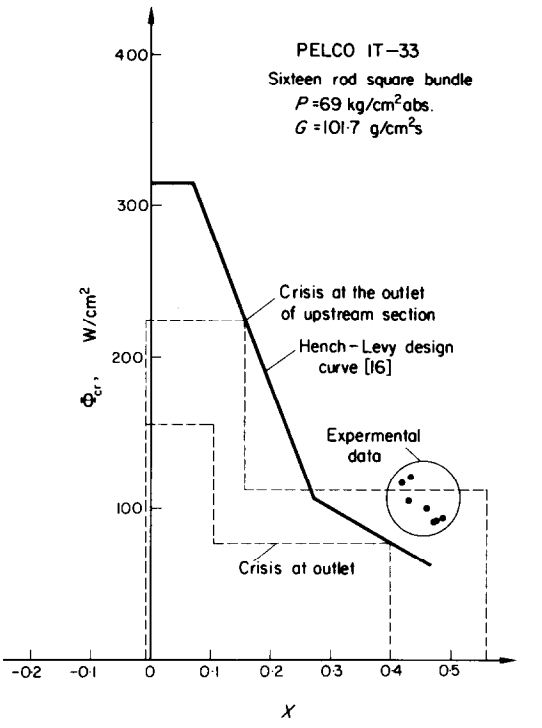

FIG. 8. Critical heat flux prediction (Hench–Levy design curve) for crisis occurring at outlet and outlet of upstream section.

stant pressure, mass flowrate, geometry. The following equation can therefore be written:

$$f(X_{cr}, L_{S,cr}) = 0.$$

[11] gives the function f as well as its dependence from the other involved parameters. Figure 7 shows the power increase which should be necessary to bring crisis to the end of the upstream portion of the test section length: as shown an increase of 25–40 per cent is necessary to achieve this.

Unfortunately the above experiments are not able to confirm this estimate neither can they give any information on the comparative validity of the global vs. local hypothesis†. For example the Hench–Levy [16] design curve (Fig. 8), which is based on the local condition hypothesis, foresees that crisis occurs first (i.e. with power increasing) at the outlet and a power increase of 45 per cent is necessary to make crisis occur also at the end of the upstream portion (the corresponding increase at this flowrate would be 33 per cent according to the CISE correlation, Fig. 7).

3.3. The heat transfer crisis always occurs on the corner rod 9 and sometimes simultaneously also on the corner rod 18 (Fig. 9): namely, at the lowest G's, 70 and 85 g/cm²s, the crisis sets in only on corner rod 9. By increasing the flowrate, the crisis spreads also to corner rod 18.

The tendency for crisis to occur on corner rod in a square-lattice rod bundle, even in the case of a uniform radial heat flux distribution, as for the present tests, has been found also elsewhere.

†According to the "local condition" hypothesis heat transfer crisis can be described by an equation which is independent from the axial flux shape and which relates the local quality to the local heat flux, i.e.: $f(X_{cr}, \phi_{cr}) = 0$

In the tests carried out some years ago at General Electric [3] with a 9 rod bundle and with a uniform radial power distribution, the crisis always occurred on the corner rod. The same tendency occurs for the tests carried out more recently on a 16 rod bundle at Columbia University [15].

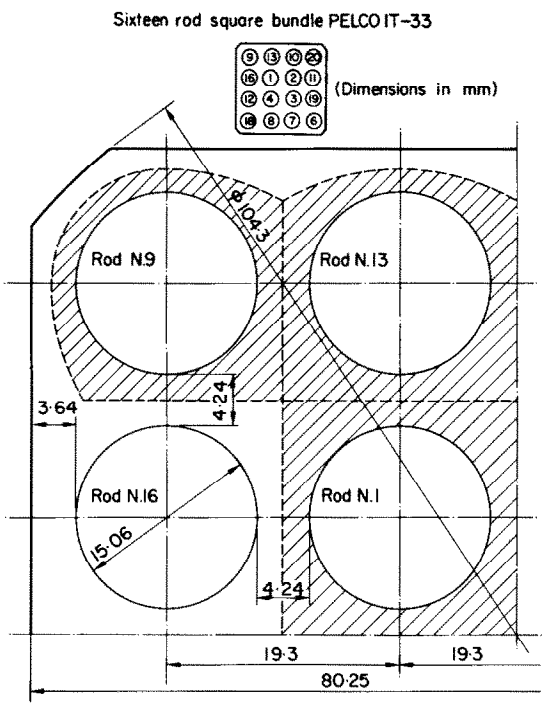

FIG. 9. Subchannels in the PELCO sixteen rod bundle.

This tendency can be found also for other bundle geometries, always with uniform radial heat flux distribution, such as for example for a 19 rod bundle [17] although the experimental evidence is less clear than with the square lattice bundles.

The tendency for crisis to set in on some particular rod in the case of a uniform radial heat flux distribution further confirms that the so-called "uniform thermohydraulic conditions hypothesis", underlying most of the presently available critical heat flux correlations for rod bundles [12, 13, 18], is inadequate. According to this hypothesis [19], with a uniform radial power distribution (i.e. among the rods) crisis occurs simultaneously (for example by increasing power, all other conditions being kept constant) on all rods,† which, as stated, is in contrast with the above results.

The above experimental results are instead in agreement with the approach proposed by CISE for critical heat flux prediction in complex geometries [11, 19]. It is based on the assumption that heat transfer crisis is described by the same equation in round tubes, annuli and rod bundles provided a suitable subchannel division is taken into account in the case of complex geometries. Analogously to some treatments made in single phase flow theory, the subchannel considered surrounds any solid surface and is ideally divided from the other subchannels by the shear stress surface (Fig. 9). The equivalent diameter is given by:

$$D_i = \frac{4\Omega_i}{p_i}$$

where Ω_i is the area and p_i the solid surface perimeter of subchannel i.

In the case of rod bundles it seemed reasonable to assume that zero shear stress surface be coincident with the surface equidistant from the various solid surfaces even though this sounds rather approximate: the limited number of available data—for square lattice rod bundle—seem to confirm the validity of the assumption, if the zero shear stress surface coincides with the maximum velocity surface.

By applying the CISE correlation for round tubes and following the above approach, the critical power of the whole bundle is given in Fig. 10 which shows that crisis should occur—as it actually does—on the corner rod (the relevant critical power values is minimum) and that a power increase of approximately 10–12

†With non-uniform radial power distribution crisis, according to this hypothesis, should occur first on the most rated rods. Thus the overall bundle critical power with non-uniform power distribution is always lower than with uniform power distribution.

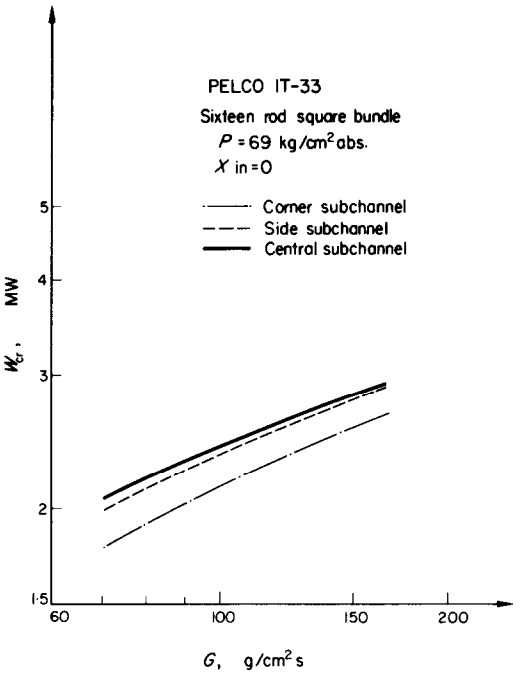

FIG. 10. Total critical power prediction for crisis on various subchannels.

per cent should be necessary to transfer the crisis on the other rods.

It would be quite an interesting exercise to check this conclusion by increasing the power of the corner rods, keeping constant the power of the other rods.

3.4. In order to test the consistency of the present critical heat flux data, the experimental results presented in [3] and in [15] and relevant to square lattice 9 and 16 rod bundles (axial and radial uniform heat flux distribution) have been compared to those obtained in the present investigation. The comparison is carried out by plotting the critical quality (i.e. the outlet quality of the subchannel—defined as in [11]—affected by the crisis) as a function of (average) boiling length for a given mass flowrate: the comparison is quite significant since all the considered rod bundles have the same equivalent diameter (= 1·26–1·30 cm) for the critical subchannel (corner rod).

As shown in Fig. 11 all the experimental data seem to be quite consistent although those obtained during the present investigation lie in a

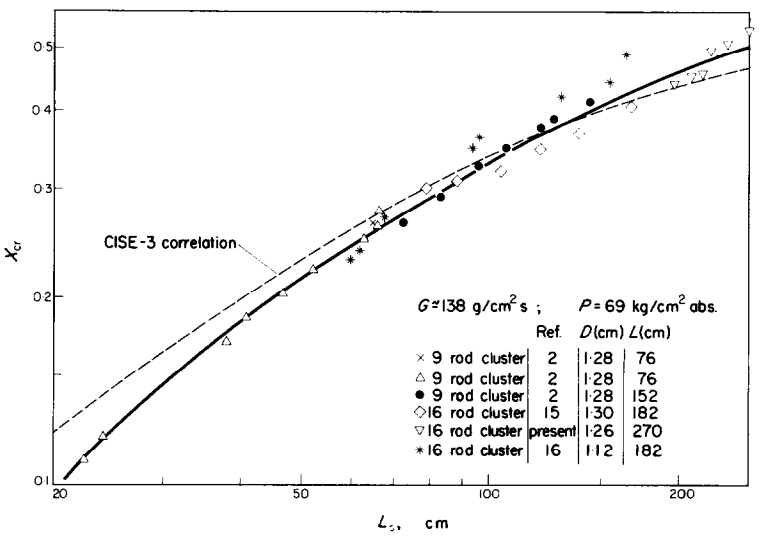

FIG. 11. Comparison between square lattice rod bundle data coming from different sources.

higher length region and therefore cannot be compared directly with the other ones: however the trend suggests that the data should be also consistent with the other ones.†

The 16 rod bundle data reported in [16] for which the critical subchannel has a smaller equivalent diameter (1·12 cm) are also presented. They lie a little above the other data, as expected.

3.5. The whole set of data (54 points) is compared with CISE-3 correlation [11] taking into account the axial power distribution; i.e. by using this correlation under the general form:

$$X_{cr,i} = f(L_{S,cr}, \text{etc.})$$

where $L_{S,cr}$ is the average boiling length, $X_{cr,i}$ is the critical quality of the critical subchannel. As stated, the crisis is predicted at the outlet and in correspondence of the corner rod, in agreement with experimental data.

Quantitatively, as it can be seen in Fig. 12, the predicted values are lower than the experimental ones from zero to 30 per cent (+13 per cent as mean error, 14·6 as root mean square error). Moreover the influence of specific mass flowrate, at least for the lower G's, is not well taken into account since there appears an evident error dependence on G.

Such a discrepancy is difficult to be explained, keeping in mind that with shorter test elements the agreement was much better [11] and with a trend, for the correlation, to overestimate experimental data. A reason for the above disagreement could be due to the fact that in this range of length at the lowest flowrates, the contribution due to enthalpy exchange between subchannel which is disregarded in the CISE-3 correlation, might be significant.

The experimental data have also been compared with Macbeth's [18], Becker's [13] and Barnett's [12] correlation. The first two authors state that their correlation should be valid also

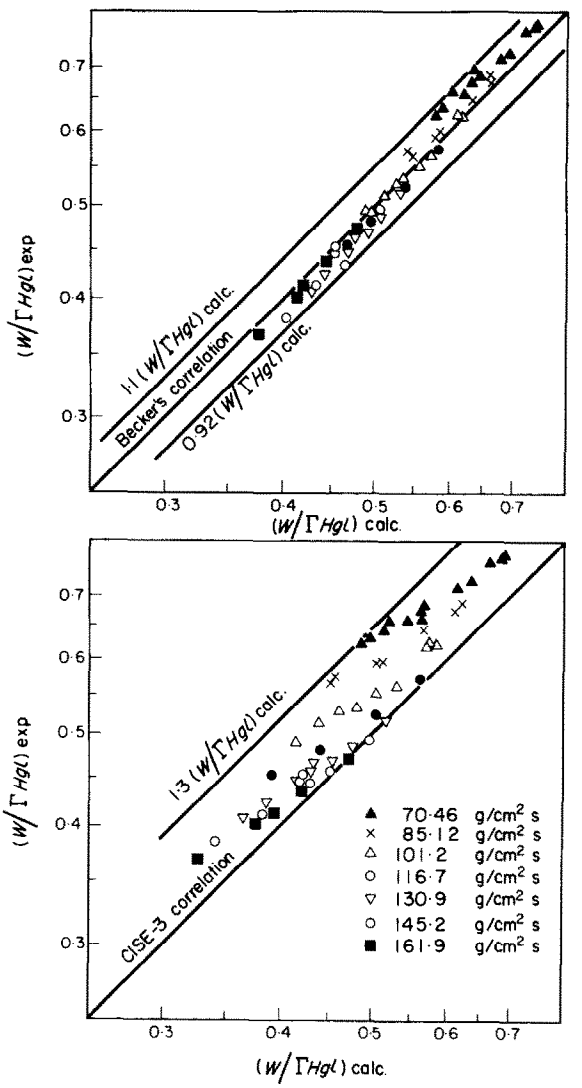

FIG. 12. PELCO IT-33 data compared with CISE-3 and Becker's correlations.

with non-uniform axial flux distribution, although they emphasize that the statement is based only on information coming from round tube data and that experiments with rod bundles should be carried out to confirm it. Barnett, instead, does not make any mention about the effect of non-uniform axial flux distribution.

As shown in Fig. 13, Macbeth's and Barnett's

†It is worthwhile mentioning that the bundle spacers for the different sets of data are not the same and the scatter of the points—which in any case is within the normal reproducibility margin of critical heat flux data—should be due mainly to this reason (see also [15]).

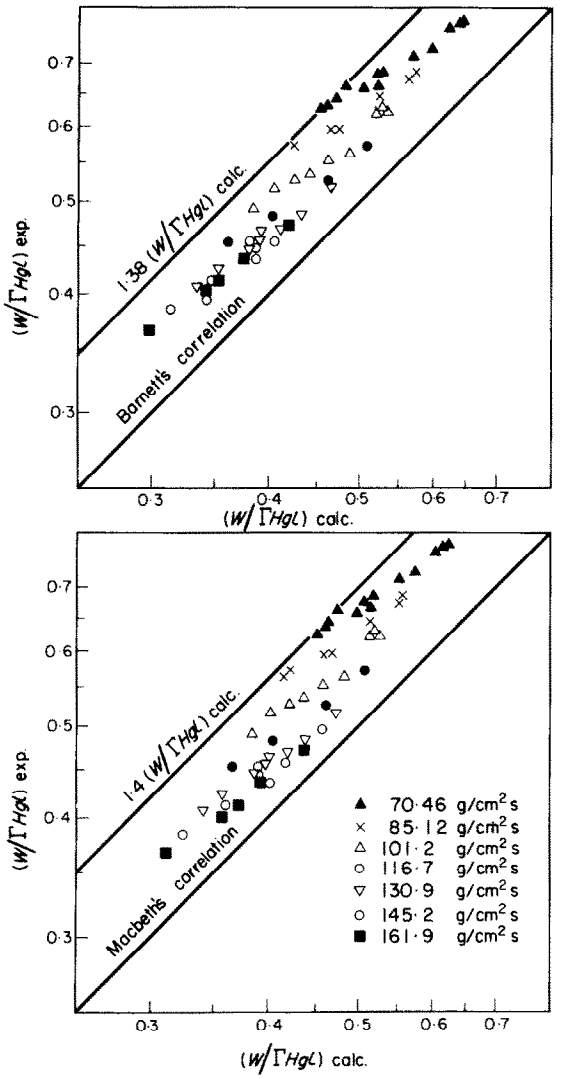

FIG. 13. PELCO IT-33 data compared with Macbeth's and Barnett's correlations.

correlations give a slightly worse prediction with respect to CISE-3 correlation (18·3 RMS error for both correlations) and again a stratification with G is evident.

Becker's correlation accurately predicts the present data (0·6 per cent as average error and 4·7 per cent an RMS error). Moreover the influence of the specific mass flowrate on critical power seems to be taken correctly into account.

4. CONCLUSIONS

The following conclusions can be drawn from the present investigation:

—with the selected stepped axial heat flux distribution heat transfer crisis occurs at the test section outlet; this in agreement with what could be inferred from available correlations;

—heat transfer crisis occurs always on a corner rod in agreement with data relevant to similar but shorter square-lattice rod bundles tested previously; this result is in contrast with the so-called "uniform thermohydraulic conditions" hypothesis on which are based most of the available critical heat flux correlations. The result is instead in agreement with the rod centered subchannel hypothesis;

—the experimental data appear to be consistent with the above mentioned data for square-lattice rod bundles; since these data were obtained with uniform axial flux distribution, the present results indicate also that the effect of non-uniform heat flux in the present tests should be negligible;

—the experimental data are satisfactorily predicted by Becker's correlation. The predictions by other correlations (Macbeth, Barnett and CISE-3) are worse and the reasons for the discrepancy are difficult to find.

ACKNOWLEDGEMENTS

The authors wish to express particular gratitude to Mr. A. Hassid for the general co-ordination of the work.

The authors wish also to thank all those who cooperated in setting-up the test assembly and in carrying out the experimental work. Particular acknowledgements are due to Messrs. N. Adorni and G. F. Germani for the design and construction of the test element, to Mr. A. Lumachi for the preparation of the related instrumentation and to Messrs. V. Tarzia and P. Casazza for the assistance with the experimental plant.

The authors are finally grateful to ENEL and in particular to the staff of Centrale Termoelettrica Emilia at Piacenza for their assistance and cooperation.

REFERENCES

1. G. BIANCHI, M. CUMO and R. EVANGELISTI, Prove termoidrauliche per elemento di combustibile a plutonio, CNEN Report TR (68) 8 EIRA-1 (March 1968).

2. J. E. HECH, Multi-rod (four-rod) critical heat flux at 1000 psia, General Electric Report GEAP 4358 (September 1963).
3. J. E. HECH and R. F. BOEHM, Nine rod critical heat flux investigation at 1000 psia, General Electric Report GEAP 4929 (January 1966).
4. K. M. BECKER, I. FLINTA, G. HERNBORG, O. NYLUND, L. NILSSON and A. JENSEN, Experimental studies of burnout conditions in vertical channels. A.B. Atomenergi Report, S-387 (June 1968).
5. A. HASSID, R. RAVETTA and L. RUBIERA, IETI-3: an out-of-pile facility for heat transfer tests of full scale reactor power channels cooled with evaporating water, *Energia Nucleare* **17**, 347 (June 1970).
6. Progetto e costruzione di un elemento a fascio di 16 barre per prove termoidrauliche interessante lo sviluppo di un elemento combustibile a plutonia, CISE Report PELCO N. 1 (October 1968).
7. D. H. LEE and J. D. OBERTELLI, An experimental investigation of burnout with forced convection high pressure water, Symposium on Boiling Heat Transfer in Steam Generating Unit and Heat Exchangers, Paper 9. Manchester (September 1965).
8. N. ADORNI, A. AZZONI, G. GERMANI, A. LUMACHI and G. MISANI, Seven rod clusters for heat transfer and pressure drop experiments: design, construction and instrumentation, CISE Report R-261 (January 1969).
9. N. ADORNI, A. AZZONI, G. GERMANI, A. LUMACHI, A. MARELLI and G. MISANI, Test element for critical heat flux, pressure drop and density measurements: 19 clustered rods, maximum design power 5·5 MW, CISE Report R-267 (July 1968).
10. S. BERTOLETTI, C. LOMBARDI and M. SILVESTRI, Heat transfer to steam–water mixtures, CISE Report R-78 (January 1964).
11. G. P. GASPARI, A. HASSIS and G. VANOLI, Critical heat flux (CHF) prediction in complex geometries (annuli and clusters) from a correlation developed for circular conduits, CISE Report R-276 (June 1968).
12. P. G. BARNETT, A correlation of burnout data for uniformly heated annuli and its use for predicting burnout in uniformly heated rod bundles, UKAEA Report AEEW R-463 (September 1966).
13. K. M. BECKEN, A correlation for burnout predictions in vertical rod bundles, AB Atomenergi Report S-349 (June 1966).
14. N. ADORNI, G. GERMANI and A. LUMACHI, Design and construction of a 16 rod square bundle for critical heat flux and pressure drop measurements with steam–water mixture, CISE Report PELCO No 3 (October 1969).
15. E. JANSSEN, F. A. SCHRAUB, R. B. NIXON, B. MATZNER and J. F. CASTERLINE: Sixteen-rod heat flux investigation, steam-water at 600 to 1250 psia. Paper presented at the Winter Annual Meeting of the ASME, Los Angeles (November 1969).
16. S. ISRAEL, J. F. CASTERLINE and B. MATZNER, Critical heat flux measurements in a 16-rod-simulation of a BWR fuel assembly, ASME Paper No 68-WA/HT-16.
17. G. P. GASPARI, A. HASSID, R. RAVETTA and L. RUBIERA, Heat transfer crisis and pressure drop with steam–water mixtures in a nineteen uniformly heated rod bundle, CISE Report R-264 (September 1968).
18. R. V. MACBETH, Burnout analysis. Part 5: examination of published world data for rod bundles, UKAEA Report AEEW R-358 (June 1964).
19. G. P. GASPARI, A. HASSID and G. VANOLI, Some considerations on critical heat flux in rod clusters in annular-dispersed vertical upward two-phase flow, Paper presented at the International Heat Transfer Conference. Versailles (September 1970).
20. E. JANSSEN, Two-phase flow structure in a nine rod channel, steam–water at 1000 psia, General Electric Final Summary Report HEAP 5480 (June 1967).

RÉSULTATS SUR LE TRANSFERT THERMIQUE CRITIQUE POUR UN MÉLANCE EAU-VAPEUR DANS UN FAISCEAU À SEIZE BARRES

Résumé—On présente les résultats expérimentaux obtenus dans le programme PELCO sur le transfert thermique critique (54 points) avec écoulement vertical ascendant d'eau bouillante dans un faisceau carré à seize barres. Les expériences de transfert thermique sont menées dans l'opération CISE IETI-3 sous les conditions suivantes:

Géométrie: (1) disposition carrée des seize barres
(2) diamètre des barres: 1,51 cm
(3) Longueur globale chauffée: 270 cm
distribution radiale de puissance: uniforme
distribution axiale de puissance: 2 échelons (ϕ en amont = 2 ϕ en aval)

($L_{\text{en amont}} = 104$ cm)

débit massique: de 70 à 160 g/cm²s (sept valeurs)
eau sous-refroidie à l'entrée (sous refroidissement de 5° à 75°C) pression moyenne dans la section expérimentale: 69 kg/cm² abs.

On donne une description brève concernant à la fois l'élément expérimental et le plan d'expériences. On conduit aussi une courte discussion sur les résultats de puissance critiques et une comparaison avec les prédictions de quelques formules utilisables.

KRITISCHE WÄRMEÜBERGANGSDATEN BEI EINEM DAMPF-WASSER-GEMISCH IN EINEM BÜNDEL AUS 16 STÄBEN

Zusammenfassung—Die Daten über die Wärmeübergangskrisis (54 Punkte) aus Experimenten unter dem PELCO-Programm an vertikaler Aufwärtsströmung von siedendem Wasser in einem Bündel von 16 Stäben im Viereck werden vorgelegt.

Die Experimente wurden mit der CISE-IETI-3-Wärmeübertragungsanlage durchgeführt unter den folgenden Bedingungen:

Geometrie: (1) 16 Stäbe im Viereck
(2) Stabdurchmesser: 1,51 cm
(3) Gesamte beheizte Länge: 270 cm

Radiale Energieverteilung: gleichförmig

Axiale Energieverteilung: zweistufig ($\phi_{\text{Aufwarts}} = 2\,\phi_{\text{Abwarts}}$; $L_{\text{Aufwarts}} = 104$ cm)

spezifischer Massenstrom: 70–160 g/cm^{2}s (sieben Werte)

Unterkühlung am Eintritt: (5° bis 75°C)

Durchschnittlicher Druck in der Teststrecke: 69 kg/cm^2 abs.

Es wird eine kurze Beschreibung des Testelementes und des experimentellen Aufbaues gegeben.

Eine kurze Diskussion der Ergebnisse bei der kritischen Wärmestromdichte und win Vergleich mit den Voraussagen nach einigen verfügbaren Beziehungen schliessen sich an.

КРИЗИС ТЕПЛООБМЕНА В ПАРОВОДЯНОЙ СМЕСИ В ПУЧКЕ ИЗ ШЕСТНАДЦАТИ СТЕРЖНЕЙ

Аннотация—Приводятся экспериментальные данные, входящие в программу исследований PELCO, по кризису теплообмена (54 точки) для вертикального восходящего потока кипящей воды в квадратном пучке из шестнадцати стержней.

Эксперименты проводилиср на теплообменной установке CISE IETI—3 при следующих условиях:

геометрия: 1. Квадратный пурек из 16 стержней:
2. Диаметр стержня—1,51 см;
3. Общая длина нагрева: 270 см

радиальное распределение мощности—равномкрное

осевое распределение мощности—двухступенчатое

($\phi_{\text{восход.}} = 2\phi_{\text{исход.}}$; $L_{\text{восход.}} = 104$ см)

удельный массовый поток: 70–160 г/см^2 (семь значений)

температура недогрева воды на входе: (недогрев от 5 до 75°)

среднее давление в рабочем участке: 69 кг/см^2 (абс.)

Дается краткое описание устройства рабочего участка и экспериментальной установки.

Приводятся также некторые результаты по критической мощности, которые сравниваются с расчетами, полученными с помощью некоторых известных корреляций.